RSC Advances

Interaction of bio-relevant thio-ether and thiols with dinuclear Pd(II) complex: Their kinetics, mechanism, bioactivity in aqueous medium and molecular docking

Journal:	*RSC Advances*
Manuscript ID:	RA-ART-11-2014-014881.R2
Article Type:	Paper
Date Submitted by the Author:	06-Jan-2015

Complete List of Authors:	Misra, Koyel; National Institute of Technology Durgapur, Chemistry Ghosh, Goutam; National Institute of Technology Durgapur, Chemistry Mitra, Ishani; National Institute of Technology Durgapur, Chemistry Mukherjee, subhajit; National Institute of Technology Durgapur, Chemistry Reddy, Venkata; National Institute of Technology Durgapur, Chemistry Linert, Wolfgang; Vienna University of Technology, Institute of Applied Synthetic Chemistry Misini, Bashkim; Vienna University pf Technology, Applied Synthetic Chemistry K, Jagadeesh C Bose; National Institute of Technology Durgapur, Bio-Tech Mukhopadhyay, Sudit; National Institute of Technology Durgapur, Bio-Tech Moi, Sankar; National Institute of Technology, Durgapur, Chemistry

Journal Name

RSCPublishing

ARTICLE

Interaction of bio-relevant thio-ether and thiols with dinuclear Pd(II) complex: Their kinetics, mechanism, bioactivity in aqueous medium and molecular docking

Cite this: DOI: 10.1039/x0xx00000x

Received 00th January 2014,
Accepted 00th January 2014

DOI: 10.1039/x0xx00000x

www.rsc.org/

Koyel Misra[a], Goutam Kr. Ghosh[a], Ishani Mitra[a], Subhajit Mukerjee[a], Venkata P. Reddy[a], Wolfgang Linert[b], Bashkim Misini[b], Jagadeesh C Bose. K[c] , Sudit Mukhopadhyay[c] and Sankar Ch. Moi[a]*

Abstract

The kinetics of interaction between $[Pd(pic)(OH)]_2(ClO_4)_2$, **2** (pic= 2-aminomethylpyridine) with the selected ligands (L): DL-methionine (DL-meth), L-cysteine (L-cys) and N-acetyl-L-cysteine (N-ac-L-cys) have been studied under pseudo-first order condition using stopped-flow spectrophotometer in aqueous medium as a function of [complex **2**] as well as [ligand], pH, and temperature at constant ionic strength. The ligand dependent second order reaction is found to take place in two consecutive steps in accordance with the rate law, $k_{(obs)} = k_1[L]^2$ in which all these three reactions follow the third order kinetics. The first step of the reaction is dependent, while the second step is independent of [ligand] in all the cases. The activation parameters, $\Delta H^{\ddagger}$ and $\Delta S^{\ddagger}$ for the two-step reactions are evaluated from Eyring equation. An associative mode of activation (an associative mechanism) in the transition state along is proposed for all these substitution processes. Complex **2** and its substituted products $[Pd(pic)DL\text{-}meth]^+$ **3**; [Pd(pic)L-cys] **4**; and [Pd(pic)N-acL-cys] **5** are characterized by UV-Vis, FT-IR, 1H-NMR and ESI-Mass spectroscopic method. Complex **2** - **5** show remarkable anticancer property on HeLa cell of about 70% at high concentration when compared to cis-platin and observed antibacterial property on both the gram positive (Bacillus subtilis) and gram negative (E.coli Dh5α) bacteria. In addition, DNA interaction with plasmid DNA is observed and computational molecular docking studies were carried out with an aim to establish the binding mode of complex **2** with B-DNA.

Key Words: Kinetics and mechanism, Di-μ-hydroxodipalladium(II) dimer, Third order reaction, Anticancer property, Antibacterial property, DNA-binding, Molecular docking

Introduction

Thiol or thio-ether bonded Pd(II) and Pt(II) complexes are biologically significant because of their applications as drug reservoir[1] and are currently under study as chemoprotectant in platinum-based chemotherapy. Platinum sulfur adducts could perhaps serve as a drug reservoir for platination at DNA. Although thousands of platinum complexes have been discovered as antitumor agents, only very few are sufficiently promising in this regard[2,3]. *Cis*platin is still one of the most widely used anticancer drug in the world, although its high activity is associated with severe side effects[4]. Binding of *cis*-platin with intracellular thiols is known to be responsible for its renal toxicity and associated side effects like nephrotoxicity, neurotoxicity, ototoxicity and gastrointestinal toxicity[5-7]. To overcome these drawbacks, researchers are trying to design safer drugs through a better understanding of ligand exchange and DNA-platination[8-10] reactions. The interaction of platinum

complexes with DNA is thought to be responsible for the antitumor activity, but there are many other potential bio-molecules (proteins and peptides) which can react with the platinum complexes[1,3,9]. Sulfur containing biologically important molecules play a significant role in the metabolism of platinum-based antitumor complexes and these S-donor ligands are available for kinetic and thermodynamic competition[1,7] with DNA. On the basis of the remarkable analogy of palladium(II) with the platinum(II) chemistry, a variety of Pd(II) complexes[11] have been proved as useful models to provide a more fitting picture of the thermodynamic and kinetic aspects of the reactions closely related to the platinum(II) complexes. Many non-platinum complexes[12] have been synthesized and tested, of which few Pd(II) complexes show considerable antitumor activity[13-16] in tumor cells with low resistance and low side effects. Mononuclear Pt(II) complex[17] $Pt(pic)(H_2O)_2]^{2+}$ with interesting spectator ligand (2-aminomethylpyridine) having σ donor and π acceptor property and other few mononuclear Pd(II) complexes[18-19] as well as dinuclear Pd(II) complexes[12] have shown good antitumor activity. Our interest is to investigate the kinetics and bioactivity of the dinuclear complex[20], $[Pd(pic)(OH)]^{2+}$ at pH 6.5 with sulfur donor ligands and their bioactivity study, which has not been studied so far.

Experimental

Physical measurements

Elemental analyses were carried out on a Perkin-Elmer 2400 series-II CHNS Analyser**.** Kinetic measurements in the UV region were carried out with a high-speed stopped-flow spectrophotometer (Applied Photo-physics SX.18 MV-R) equipped with a diode array detector and a Shimadzu TB thermo-bath (accuracy ±0.1˚C) running under SX.18 MV kinetic package. All the kinetic measurements were carried out at pH 6.5 and were performed under pseudo-first-order conditions, at least a 10-fold excess of the ligand concentrations. The Fourier transform infrared spectra of the ligands and the complexes were recorded on Thermo Nicolet-iS-10 spectrometer in wave number region (4,000-400 cm^{-1}, KBr disk) and 400-100 cm^{-1} recorded using CsI disk. The electronic spectra were recorded on Shimadzu-1601 spectrophotometer in the wave length range 200-800 nm attached with thermoelectric cell temperature controller (model TCC-240A), accuracy ± 0.1°C. NMR spectra were recorded with a Bruker-400 Ascend spectrometer using D_2O or DMSO-D_6 as solvent. ESI Mass spectra were carried out in Waters Qtof Micro YA263 Mass spectrometer in DMSO solvent. HEX software was used for molecular docking of complex 2 with B-DNA (from protein data bank).

Reagents and Materials

All chemicals used in the kinetic and bio-activity studies were of the highest purity as available. The starting compounds $PdCl_2$ (99%), DL-methionine, L-cysteine and N-acetyl-L-cysteine were purchased from Sigma Aldrich. 2-Aminomethylpyridine (pic), $AgClO_4$, $AgNO_3$ and potassium dihydrogen orthophosphate were purchased from Alfa Aesar and $NaClO_4$ from Fluka. All these reagents were used without further purification. Ultra-pure water was used to prepare all kinds of solutions, and all solvents used were of analytical grade. To investigate the bioactivity, Human cervical carcinoma cell lines (HeLa cell) were cultured in DMEM medium (Hi-Media) containing 10% FBS (Hi-Media) with antibiotic concentration 1% of penicillin/streptomycin (50 IU/ml and 500 µg/ml), respectively in CO_2 incubator with a humidified atmosphere (95% air/ 5% CO_2) at 37°C for 2 days. Cell viability was investigated by using the MTT (3- (4, 5-dimethylthiazolyl-2) -2,5-diphenyltetrazoliumbromide) colorimetric assay based on a reaction between mitochondrial enzyme dehydrogenase from viable cells with the yellow tetrazolium rings of MTT. The colour can be quantified by using the colorimetric assay on a multi-well scanning spectrophotometric method by ELISA reader (Stat Fax™® 2100 Micro plate Reader, USA).We have used bright field inverted microscope (Zeiss) to detect the survival HeLa cells.

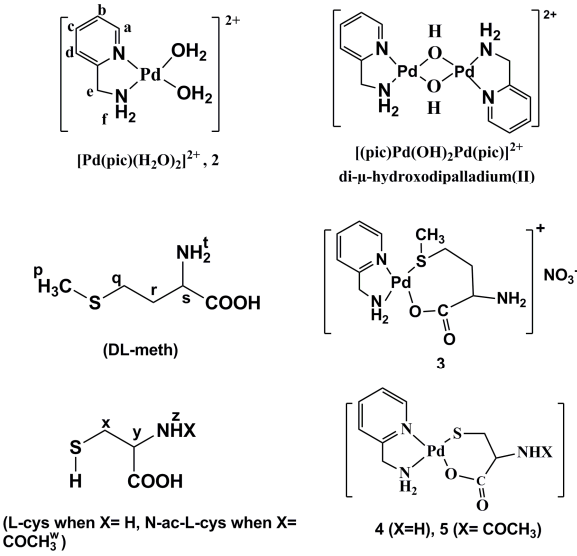

Structures of complexes and ligands

Syntheses of complexes

[Pd(pic)Cl_2] 1

[Pd(pic)Cl_2] **1** was synthesized according to literature reported procedure[21] with modifications. $PdCl_2$ (0.5 g, 2.8 m.mol) in 7 ml of water and 3 ml of HCl (37%) was heated for 30 min. The resultant

$[PdCl_4]^{2-}$ solution was cooled to 20°C. 2-aminomethylpyridine (0.292 ml, 2.7 m.mol) dissolved in 4 ml of water was added to it drop wise with stirring. A yellow precipitate appeared gradually, and the mixture was stirred for a further period of 2 h at 20 °C for completion of precipitation. The precipitate was filtered off and washed successively with water, ethanol and diethyl ether and then dried in vacuum. Yield: 0.73 g (2.50 m.mol, 89.0%) Anal. found for $C_6H_8N_2Cl_2Pd$: C, 25.31; H, 2.72; N, 9.66; calcd.: C, 25.25; H, 2.82; N, 9.81. Yield of complex **1** in the form of a light yellow powder was 0.74 g (2.29 m.mol; 91%). Elemental analysis (atom %) for $C_6H_8Cl_2N_2Pd$ **1**: found; C, 25.27; H, 2.69; N, 9.65 (calc; C, 25.25; H, 2.82; N, 9.81). Electronic absorption spectrum of **1** in DMSO, (λ_{max}/ nm (ε/$M^{-1}cm^{-1}$): 272(2067); Selected IR frequencies (KBr disk, cm^{-1}): 2970(s), 1633(s), 1614(s), 1380(s), 1110 cm^{-1} and 941cm^{-1}.

$[Pd(pic)(H_2O)_2](ClO_4)_2$ 2

The diaqua complex **2** was obtained in solution by the method of Hay and Basak[21] by stirring the chloro complex **1** with two equivalents of $AgClO_4$ in water at 60 °C for 2h. The solution was kept in dark overnight and the white AgCl precipitate was removed by filtration. To ensure that no trace of Ag^+ ion remained in the solution, the pH was adjusted to 12-13 and the black Ag_2O precipitate was filtered off. The pH of the diaqua complex solution was adjusted at 3.0 to prevent hydrolysis and freshly prepared diluted solutions of the same were used for kinetic measurements. Another aliquot of complex **2** was prepared from **1**, as NO_3^- salt $[Pt(pic)(H_2O)_2](NO_3)_2$ using $AgNO_3$ solution for hydrolysis (same method as $AgClO_4$) for the purpose of bioactivity studies.

Electronic absorption spectrum of **2** in H_2O, (λ_{max}/ nm(ε/$M^{-1}cm^{-1}$): 264 (1809); Selected IR frequencies (KBr disk, cm^{-1}): 3434(br), 3045(s), 2935(s), 1637(s), 1614(s), 1380(s), 1110(s), 1078(s), 630(s), 507(s) and 420(s). The ^{1}H NMR (400 MHz, D_2O) data for complex (**2**): δ 8.04 (t, J = 5.6, J=3.2,1H), δ 8.0 (d,d, J = 8.0, J = 1.2, 1H), δ 7.52 (d, J = 6.4, 1H), δ 7.4 (d, J = 8.4, 1H), δ 4.61 (s, 2H), δ 4.37 (s, 2H), δ 1.79(s) 2H.

Syntheses of complex 3-5

Substituted product complexes $[Pd(pic)DL\text{-}meth]^+(NO_3^-)$ **3**; [Pd(pic)L-cys] **4**; and [Pd(pic)N-acL-cys] **5** were synthesized from complex **2** by mixing the ligands, DL-meth, L-cys and N-ac-L-cys in 1: 1 molar ratio at pH 6.5 respectively for their characterization. Electronic absorption spectrum of **3** in H_2O (λ_{max}/ nm(ε/$M^{-1}cm^{-1}$): 234 (7393); Selected IR frequencies (KBr disk, cm^{-1}): 3427-3313(br), 3246-3185(br) 2930-2900(br), 1627(s), 1110(s), 665(s), 509(s), 436(s) and 331(s). ^{1}H NMR (400 MHz, DMSO-D_6) data for complex (**3**) (SI Fig S1) : δ 8.25 (d, J = 6,0, 1H^a), δ 8.15 (m, J = 5.6, 1H^c), δ 7.67 (d, J = 8.0, 1H^d), δ 7.55 (t, 1H^b), δ 5,5 (br, , 2H^t), δ 4.85 (t, 2H^f), δ 4.2 (s, 2H^e), δ 3.80 (m, 1H^s), δ 2.7 (m, 1H^q), δ 2.66 (m, 1H^q), δ 2.03 (s, 3H^p) and δ 1,9 (m, 2H^r). ESI-Mass spectrum of **3** shows molecular ion peak at m/z 362.05 in DMSO solvent.(SI Fig S2)

Electronic absorption spectrum of **4** in H_2O (λ_{max}/ nm(ε/$M^{-1}cm^{-1}$): 258 (572); Selected IR frequencies (KBr disk, cm^{-1}): 3431-3363(br), 3161(br), 2940-2900(br), 1602(s), 1386(s), 1072(s), 644(s), 501(s), 439(s) and 312(s) . ^{1}H NMR (400 MHz, δ in ppm, DMSO-D_6) data for complex **4**: δ 8.47 (d, J = 4.8, 1H^a), δ 7.85 (t, J = 1.6, J = 1.2, 1H^c), δ 7.40 (t, J = 8.0 J = 5.6, 1H^d), δ 7.37 (d, J = 7.2, 1H^b), δ 4.2 (s, 2H^f), δ 3.9 (d, J= 4.0, 2H^x), δ 3.59(d,d, J=3.6, J=3.0, 2H^y); δ 3.07(m 2H^z); δ 2.94 (m, 1H) (SI Fig. S3). ESI-Mass spectrum of **4** shows molecular ion peak at m/z 333.13 in DMSO solvent.

Electronic absorption spectrum of complex **5** in H_2O (λ_{max}/ nm (ε/$M^{-1}cm^{-1}$): 265 (717); Selected IR frequencies (KBr disk, cm^{-1}): 3423-3361(br), 3170(br), 2933-2905(br), 1674(s), 1610-1600(br), 1384(s), 1072(s), 655(s), 530(s), 460(s) and 306(s). ^{1}H NMR (400 MHz, DMSO-D_6) data for complex **5**: δ 8.10 (d, J = 6.0, 1H), δ 8.0 (s, 1H), δ 7.59 (d, J = 10.0, 1H), δ 7.49 (d, J = 6.0, 1H), δ 7.44 (d, J = 6.8, 1H), δ 4.84 (d, J=4.4, 2H); δ 4.27 (s, 2H), δ 4.37 (s, 2H), δ 2.01(t, J=3.2, J=4.8, 2H) δ 1.85(s) 3H(SI Fig. S4). ESI-Mass spectrum of **5** shows molecular ion peak at m/z 375.23 in DMSO solvent.

Synthesis safety note

Perchlorate salts of transition metals should be handled cautiously as these are hazardous and explosive upon heating. No explosion event was encountered in the present study.

Kinetic investigation

Kinetic study of Pd(II) complexes with bidentate ligands (N,N) is still a promising area of research due to their antitumor property[23] and interesting kinetic behaviour. The critical analytical concentration for the ligands ([ligand] = 2.62×10^{-3}M) and metal complex **2** ([complex **2**] = 2.62×10^{-4} M) were determined by UV-Vis spectroscopy at pH 6.5 at which the kinetic investigations were carried out. The spectral changes resulting from the mixture of complex **2** and solutions of DL-meth, L-cys and N-ac-L-cys (Fig.1) (see SI in Fig. S5) were recorded over the wavelength range 200-600 nm to establish a suitable wavelength at which kinetic measurements could be performed. Complex **2** and the ligands were mixed individually at pH 6.5 and the mixtures were set at 60 °C for 48 h. The resultant solutions of **3, 4** and **5** showed characteristic peaks at λ

$_{max}$ 234, 258 and 265 nm respectively with maximum absorbance difference with the complex **2**. The kinetic measurements of the reactions were monitored with a stopped-flow spectrometer at pH 6.5 at their respective wavelengths. It was assumed that the absorbance difference between complex **2** and the individual mixtures **3, 4** and **5** was a function of the amount of complex formed (Fig. 1.) (Fig. SI in S5).

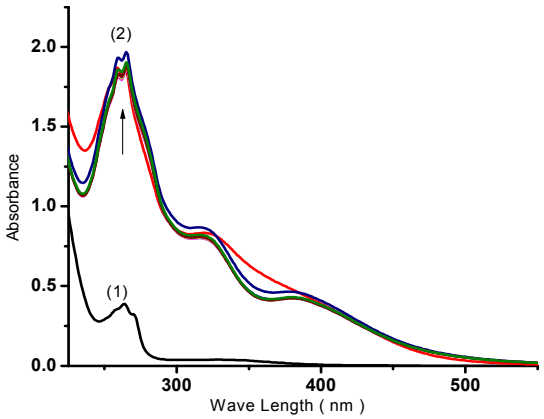

Fig.1: Spectral difference between complex $[Pd(pic)(OH)]_2^{2+}$ and product 2 (1) $[Pd_2(pic)_2(OH)_2]^{2+} = 2.62\times10^{-4}$ M, (2) $[Pd_2(pic)_2(OH)_2]^{2+} = 2.62\times10^{-4}$ M, [L-cysteine] = 2.62×10^{-3} M pH = 6.5, cell used 1 cm quartz

The reactions were initiated by mixing equal volumes of complex **2** and individual ligand solutions directly in the stopped-flow instrument and were followed for at least eight half-lives. The interaction of complex **2** with the ligands were followed under pseudo-first order condition with [ligand] ranging from 2.62×10^{-3} to 13.1×10^{-3} M (10-50 fold) and the [complex **2**] was fixed at 2.62×10^{-4} (M). The reactions were carried out at pH 6.5 and at temperatures 15, 25, 35 and 45 ^{o}C (ionic strength 0.1 M $NaClO_4$). All kinetic runs could be fitted to a double exponential function (SI Fig. S6), employed to fit the kinetic traces. Potassium dihydrogen orthophosphate/sodium hydroxide buffer was used to prevent any change of pH throughout the reaction.

Bioactivity study

Test microorganisms and bacterial culture Suspension preparation

Antibacterial activity of complex **2-5** were studied on both gram positive *Bacillus subtilis* and gram negative *Escherichia coli* model organisms. Bacterial culture suspensions were prepared by the direct colony method. The isolated single colonies were taken directly from the LB agar plate and sub cultured in 100 ml of sterile LB broth (Himedia) and incubated at 37ºC for 12 hours overnight. The turbidity of initial LB broth was adjusted to zero and this was measured for colony forming units (CFU) to estimate the bacterial count and used as constant control for the entire experiment. The main aim of the study is to find out the antibacterial activity of complex **2-5**.

***In vitro* antibacterial activity by Tube dilution method**

Antimicrobial activity of complex **2-5** was tested by determining the turbidity colorimetric measurement by using tube dilution method[24]. The set of 10 sterile tubes was prepared by dispensing the LB broth each tube to attain desired volume. The blank and control were maintained for each setup. The final concentration of compounds ranges from 0.05 µM to 0.25 µM was used. A 10 µl of diluted bacterial suspension was inoculated to each tube to give a final concentration of 5×10^5 CFU/ml. The same steps were carried for three sets. After incubation, optical density at 600 nm over the corresponding blank, were noted to determine the number of cells in each tube[25]. Tetracycline was used as a positive control. Each test included growth control and sterility control. All tests were performed in triplicate and cell count by turbidimetry and % of inhibition were calculated. Minimal bactericidal growth was determined as inhibition by observing the turbidity absorption pattern in LB broth. The average values of the absorbance by *Escherichia coli* and *Bacillus subtilis* at 600 nm were considered for plotting the graph by Graph Pad Prism software.

***In vitro* cytotoxic effect of complex 2-5 on HeLa cell**

Cells, culture condition and Cell counting

The cells were cultured using 96-well plates and maintained at 37 ^{o}C in DMEM with 10% FBS and appropriate antibiotics in 5% CO_2 incubator. Cell viability was investigated by using the MTT colorimetric assay[25,26].

In vitro cytotoxicity assay was carried out in culture plates. To investigate the effect of complexes **2** to **5** on the propagation of HeLa cells, the growth panorama of cancer cells was calculated. From cell lines, 100 µl of cell suspension which contain approximately similar number of cells were added to each well of a 96-well plate. After 24h of incubation, the cells were treated with desired concentration of Pd(pic) complexes. Cisplatin [Cisgland from Gland Pharma Limited] was used as a positive control in the same concentrations[27]. The plates were incubated for 24 hrs with both positive and negative controls. After that 20 µl MTT (5mg/ml in PBS; Phosphate buffered saline) was added to each well and incubated for another 3hrs. Then the media was carefully removed

and 150 µl of DMSO was added to each well to dissolve the blue formazan product. The absorbance of this product was measured at 540nm, using ELISA (Enzyme-linked immunosorbent assay) plate reader (Stat Fax ^{TM} ® 2100 Microplate Reader, USA).

Results and Discussion

Spectroscopic analyses

The bonding nature of complex **2** and its substituted product complex **3**-**5** were characterized by different spectroscopic methods.

UV/Vis spectra

UV/Vis spectra of the substituted products **3**, **4** and **5** shows λ_{max} at 234, 258 and 264 nm with hypsochromic as well as hyperchromic shift compared to the complex **2** due to n →π* and π→π* transitions of the respective ligands in the complexes.

Infrared spectra

Each of the ligands (DL-meth, L-cys, and N-ac-L-cys) have three potential coordinating sites (S, O, N) towards the metal center. FT-IR analysis has been used to determine the structures of complex **2** and substituted metal complex **3**-**5**. The assignment of the most important bands in the IR spectra (Fig. S7-S14 in SI) of complex **3**-**5** is based on the data for DL-meth, L-cys and N-ac-L-cys[28]. νS-H stretching frequency of L-cys and N-ac-L-cys at 2565- 2520 cm^{-1} region disappeared in its corresponding Pd(II) complexes [Pd(pic)L], where L= L-cys and N-ac-L-cys. It is amply clear that sulfur is the coordinating site of L-cys and N-ac-L-cys with complex **2** at pH 6.5. In case of complex **3**, -S-CH_3 str band shifted compared to the ligand itself, which supports sulfur chelation. Again, (S, O) chelation has also been suggested by M. Chandrasekharan et al. with Pd(II) and Pt(II) complexes[29]. The OH stretching bands of the carboxylic group in the free ligand[30] have low intensity, and appear at quite lower frequency 1633(w) cm^{-1} and are split into several components. A couple of strong bands, assigned to ν_{as} (COO) and ν_s (COO), appear in the spectra of the complexes at around (1612 – 1596 cm^{-1} and 1390 – 1384 cm^{-1}) respectively. It is expected that carboxylate group (-COO^-) oxygen coordinates to Pd(II)[29,31]. A similar couple of bands have been assigned for involvement of carboxylic groups of L-cys and N-ac-L-cys with Pd(II) at around similar positions (SI Fig. S9-S14). It is very difficult to assign all the vibrational frequencies but attempts have been made to specify characteristic frequencies which will support the (S, O) coordination of the ligands in their respective Pd(II) complexes. ν Pd-O, and νPd-S appear[32-35] in the range of 460-420 and 345-295 cm^{-1} respectively. No change in the strong band position δ(NH_2) around 1612 cm^{-1} in each of these complexes clearly indicate that the nitrogen of the amino group of these ligands is not a ligation site towards the Pd(II) center. Therefore, the IR spectra strongly supports coordination of (S, O) to Pd(II) in complex **3**-**5**.

^{1}H NMR spectra

The chemical shift position of –NH_2 protons remains unaltered at 5.4 ppm in complex **3** as compared to that of DL-meth, which indicates that –NH_2 is not the coordinating site to Pd(II) center. However, the position of the thio-methyl protons (-S-CH_3) changes from 1.92 to at 2.03 ppm. It clearly provides the evidence of sulfur chelation to Pd(II) followed by change in positions of other protons. More or less similar change of shift position of same protons of L-cys and N-ac-L-cys were observed in complex **4** and **5**.

ESI Mass spectra

Aqueous solution of **2** and the selected ligands were mixed separately in 1:1 molar ratio at pH 6.5, and the products complexes **3**, **4** and **5** were equilibrated at 60 ^oC for 48 h. The ESI-mass spectrum of the resulting solution **4** is shown in SI Fig. S2. The molecular ion peak at m/z 362.05 corresponds to ([Pd(pic) + DL-meth-1H^+) which confirms the proposed product to 100% abundance of the isotope peaks matched with the expected values. The other peaks appear at m/z 109.07, 261.10, and 321.05. Similarly for complex **4,** peaks are found at m/z 196.09, 214.10 and. 333.13 (molecular ion peak, 100% for Pd(pic) + L-cys-1H^+) and for complex **5**, peaks are found at m/z 109.07, 239.11 261.10, 283.09 and 375.23 (molecular ion peak, 100% for Pd(pic) + N-ac-L-cys - 1H^+).

Kinetic study

Kinetics and mechanism

The observed pseudo-first order rate constants, $k_{1(obs)}$ (SI in Table S1(A)-S3(A)) were calculated as an average value from four to six independent kinetic runs with an error limit within ± 5.0%. The acid-base equilibria (shown in Scheme 1) of complex **2** had been characterized[21] by Tobias Rau et al. fitted with their potentiometric titration data to various acid-base model. The fitted model, according to the method of calculation, was found to be consistent with the deprotonation of two coordinated water molecules as shown below.

$$[Pd(pic)(H_2O)_2]^{2+} \underset{}{\overset{K_{a1}}{\rightleftharpoons}} [Pd(pic)(H_2O)(OH)]^{+} + H^{+} \quad .....(1)$$
10-0 10-1

$$2[Pd(pic)(H_2O)(OH)]^{+} \overset{K_{dimer}}{\rightleftharpoons} [(pic)Pd(OH)_2Pd(pic)]^{2+} + 2\,H_2O \quad .....(2)$$
10-1 20-2

$$[Pd(pic)(H_2O)(OH)]^{+} \overset{K_{a2}}{\rightleftharpoons} [Pd(pic)(OH)_2] + H^{+} \quad .....(3)$$
10-1 10-2

Scheme 1. Dissociation equillibria of $[Pd(pic)(H_2O)_2]^{2+}$ complex

The pK_{a1} and pK_{a2} values of complex **2** were found to be 4.43 and 8.64 respectively[21]. Rudi van Eldik and his coworkers had studied the kinetic interaction of $[Pd(pic)(H_2O)_2]^{2+}$ with CBDCA, 5′-IMP and Inosine at pH 3.5, where the two aqua molecules were labile. Their evaluated rate constants were higher than our calculated rate constants at pH 6.5. Consequently, our proposed mechanism is also different. The $[Pd(pic)(H_2O)_2]^{2+}$ complex at pH 6.5 exists as di-μ-hydroxodipalladium(II), $[Pd(pic)(OH)_2Pd(pic)]^{2+}$ (complex **2**) (20-2) species (≈60%) in equilibrium. Hydroxoaqua species $[Pd(pic)(H_2O)(OH)]^{+}$ (10-1) (≈35%) dimerized to $[Pd(pic)(OH)]_2^{2+}$ **2** (S1 Fig. S15) at pH 6.5 without any $[Pd(pic)(OH)_2]$ formation. The hydroxoaqua species (10-1) does not involve itself in ligand substitution process directly and is ultimately transformed into complex **2** (20-2) in situ at pH 6.5 because they are in equilibrium. The complex **2** (20-2) is the exclusive reactive species towards the substitution process at pH 6.5. Kinetic study at higher pH (>6.5) was avoided because the complex solution became turbid.

The dissociation equilibria of L-cys, (similar to DL-meth and N-ac-L-cys) (with different pKa values) is shown below in Scheme **2** and the corresponding pKa'_1, pKa'_2 and pKa'_3 values[36] are 1.71, 8.35 and 10.78 at 25 ^oC respectively

$$SH\text{-}CH_2CH(\overset{+}{N}H_3)\text{-}COOH \overset{pK_{a1}'}{\rightleftharpoons} SH\text{-}CH_2CH(\overset{+}{N}H_3)\text{-}COO^- + H^+,\ pK_1' = 1.71 \quad ..(4)$$

$$SH\text{-}CH_2CH(\overset{+}{N}H_3)\text{-}COO^- \overset{pK_{a2}'}{\rightleftharpoons} {}^-S\text{-}CH_2CH(\overset{+}{N}H_3)\text{-}COO^- + H^+,\ pK_2' = 8.35 \quad ...(5)$$

$$^-S\text{-}CH_2CH(\overset{+}{N}H_3)\text{-}COO^- \overset{pK_{a3}'}{\rightleftharpoons} {}^-S\text{-}CH_2CH(NH_2)\text{-}COO^- + H^+,\ pK_3' = 10.78 \quad ..(6)$$

Scheme 2. Dissociation equillibria of L-cysteine at different pH

Thus, at pH 6.5 the ligand exists mainly as a neutral molecule and the amount of protonated form is less. Similarly, first pK_{a1} and pKa_2 values of N-ac-L-cys[37,38] and DL-meth[39] are 3.24, 9.52 and 2.24, 9.07 at 25 ^oC respectively.

Substitution reactions of complex **2** with the selected ligands (L) involves a two-step process (Scheme 3A and 3B) as represented by the equation (7).

$$[Pd_2(pic)_2(OH)_2]^{2+} + 2L \rightarrow 2[Pd(pic)L] + 2H_2O \quad \text{--------- (7)}$$

The reactions (7) were monitored at 245, 242, and 310 nm for DL-meth, L-cys, and N-ac-L- cys respectively in excess of [L] to ensure pseudo-first order conditions. The [ligand] dependence pseudo-first order rate constant $k_{1(obs)}$ (SI table S1(A)-S3(A) of the reaction is fitted as demonstrated in Fig. 2. The plot is noticeably curved, which indicates the reaction order is higher than 1 and fits with the second order kinetics with respect to the [L]. Reaction (7) follows the rate expression (8) with second order rate constants for the first step k_1 = 0.75×10^4 $M^{-2}s^{-1}$, 2.12×10^4 $M^{-2}s^{-1}$, and 0.57×10^4 $M^{-2}s^{-1}$ for DL-meth, L-cys, and N-ac-L- cys respectively at 25 ^oC.

Rate = $\{(K_{a1} \times K_{dimer})/K_{a2}[Pd(pic)(OH)]_2\}k_1[L]^2 \times$ [complex **2**] …… (8)

Where, $K_{a1} >> K_{dimer}$ and $K_{dimer} >> K_{a2}$ and K_{a1}, K_{a2} and K_{dimer} are the equillibrium constants in Scheme 1.

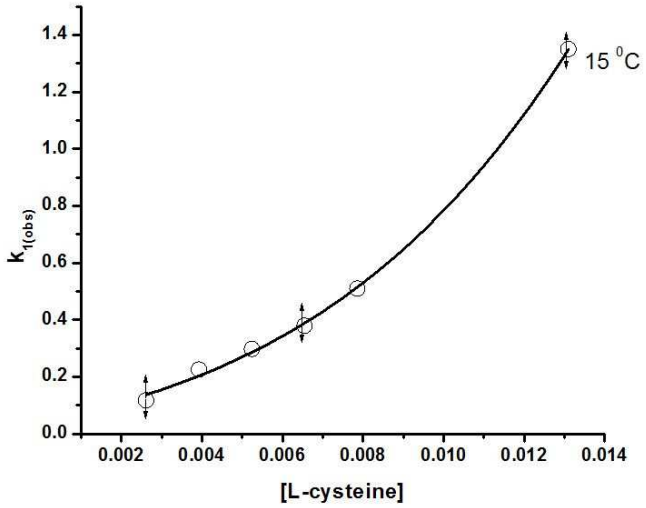

Fig. 2: Pseudo-first order rate constants k (1_{obs}) for the formation of [Pd(pic)L] as a function of $[L]^2$ (Where Nu = L-cys) at 15 ^{o}C. The curvature is drawn using the best-fit parameter of Eq. (8)

The second order reaction with respect to the incoming ligand (L) is the result of simultaneous substitution of both the bridged OH groups of complex **2** by respective S and O donor centers of the ligands (Scheme 3A and 3B). Literature survey reveals that the observed reactions are the second example of the rarely found third order kinetics[40] in Pd(II) chemistry. The k_1 values, summarized in Table 1, were determined from the average value at different points on the curve (Fig.2) at different positions and different temperatures. The second step which represents the ring closure step through oxygen chelation of the carboxylate group ($-COO^-$) is independent of [ligand].

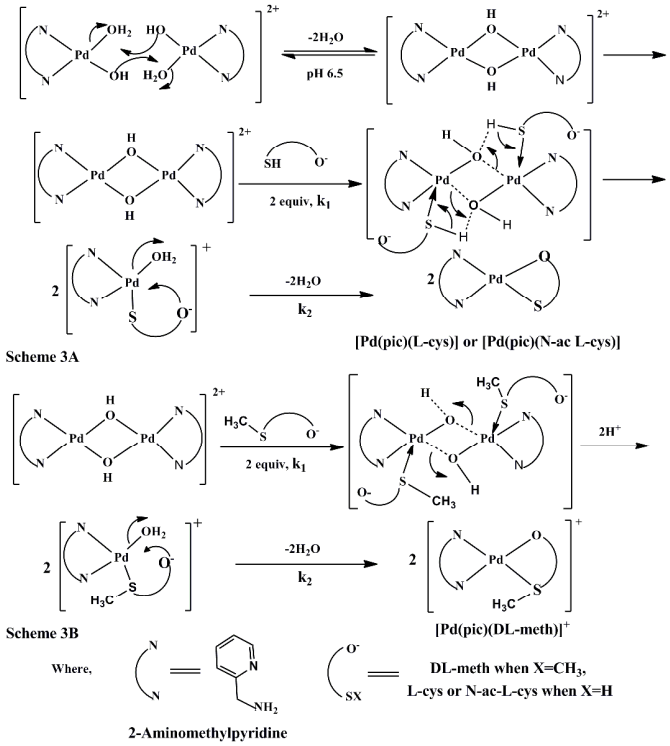

Scheme 3A and 3B: Proposed mechanism for the interaction of thiol(3A) and thio-ether(3B) with complex 2

carboxylate group of the ligands. Metal: ligand ratios were determined by Job's methods and were found to be 1 : 1 in each case (SI Fig S16). An interesting observation of the reactions is that in case of the thiols, pH of the reaction medium remains almost unchanged, whereas in the case of DL-meth an increase in pH from 6.5 to 7.13 is found which supports our proposed mechanism.

Effect of temperature on Reaction Rates

The effect of temperature on the reaction rates were studied at four different temperatures in the range of 15 to 45 °C. The activation parameters, calculated from Eyring plots **(**Fig. 3) (SI Fig. S17-S18 for DL-Meth and N-ac-L-cys) are given in Table 2 along with those for analogous systems (SI Table S4).

The large negative values of $\Delta S^{\ddagger}$ for the first and second steps indicate ordering of the reacting species and emphasize the suggested associative substitution mechanism[41,42] for the investigated complex formation. The enthalpy of activation($\Delta H^{\ddagger}$) for first and second steps for all these reactions were in fair agreement with those found for related Pd(II) complexes (Table-2) with subsequent diamine ligands[42].

Table 1. Rate constants for the reaction of (2) with different ligands at pH = 6.5 and 0.1M $NaClO_4$

Temp. (^oC)	pH	DL-meth		L-cys		N-ac-L-cys	
15	6.5	k_1 ($M^{-2}s^{-1}$)	$0.56 \times 10^4 \pm 12$	k_1 ($M^{-2}s^{-1}$)	$1.34 \times 10^4 \pm 12$	k_1 ($M^{-2}s^{-1}$)	$0.20 \times 10^4 \pm 11$
25			$0.75 \times 10^4 \pm 16$		$2.12 \times 10^4 \pm 21$		$0.57 \times 10^4 \pm 12$
35			$1.35 \times 10^4 \pm 10$		$2.81 \times 10^4 \pm 13$		$1.23 \times 10^4 \pm 19$
45			$1.88 \times 10^4 \pm 13$		$3.44 \times 10^4 \pm 17$		$1.80 \times 10^4 \pm 13$
15		k_2 (s^{-1})	4.4 ± 0.1	k_2(s^{-1})	7.90 ± 0.4	k_2 (s^{-1})	3.04 ± 0.1
25			5.25 ± 0.1		8.96 ± 0.2		3.21 ± 0.2
35			5.96 ± 0.1		10.24 ± 0.2		3.29 ± 0.1
45			6.53 ± 0.3		11.60 ± 0.3		3.40 ± 0.2

Table 2. Activation parameters

system	$\Delta H_1^{\ddagger}$ (kJ/mol)	$\Delta S_1^{\ddagger}$(JK^{-1}/mol)	$\Delta H_2^{\ddagger}$(kJ/ mol)	$\Delta S_2^{\ddagger}$(JK^{-1}/mol)
$[Pd(pic)(H_2O)_2]^{2+}$ / DL-meth	32.75±1.98	-45.51 ±6.22	4.73 ±1.10	-205.6 ±5.21
/ L-cys	21.94±1.51	-89.19 ± 5.1	5.40 ±1.10	-195.44 ±8.22
/ N-ac-L-cys	35.53±2.62	-54.52 ±3.6	1.66± 0.56	-197.31 ± 5.26

The values of the rate constant of the second step, $k_2(s^{-1})$ presented in Table 1, were calculated from $k_{2(obs)}$ values (see SI in Table S1(B)-S3(B)). The reactivity order of ligands is: L-cys >DL-meth >N-ac-L-cys. The thiol group (–SH) of L-cys forms hydrogen bonding with bridge –OH of complex **2**, which provides extra stability to outer sphere association compared to DL-meth. Slow reaction rate for N-ac-L-cys may be due to the acetyl group, which decreases the donor property of sulfur and oxygen via its electromeric effect and steric effect. Moreover, protonated form of N-ac-L-cys remains as a major species at pH 6.5 causing the reaction to be slow.

The sluggishness of the second step may be attributed to the steric retardation and lower affinity of Pd(II) towards oxygen of the

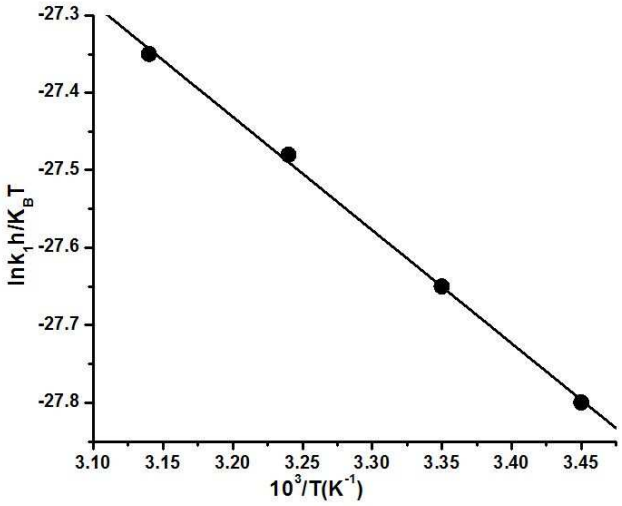

Fig. 3: Eyring plot of lnk$_1$/T vs 1/T for L-cysteine

In vitro bio-activity study

Antibacterial property

The effect of Pd(II) complexes on bacteria (gram positive and negative) was investigated by a rapid turbidometric assay with tetracycline as positive control. The results of *in vitro* antibacterial activities of the complex **2** and corresponding ligand substituted complexes **3**, **4** and **5** are shown in SI Fig. 19 and 20. The rate of growth inhibition of both kinds of bacteria was proportional to the concentration of the complexes in the media. The substituted complexes **3**, **4** and **5** do not show better inhibition as compared to complex **2** alone. Greater inhibition is observed for Gram positive *Bacillus subtilis* bacteria (SI Fig. S19) than Gram negative *Escherichia coli* (SI Fig. S20).

In vitro cyctotoxicity assay

MTT assay for anticancer property of complexes 2-5

The viability of HeLa cells was analyzed within the plates and compared with the control. As shown in Fig. 5, with increase in the concentrations of the Pd(pic) complexes, the percentage of cell survival of HeLa cells follows a descending trend line after 24 hrs incubation period. These results of *in vitro* chemo sensitivity evaluation of the cytotoxicity of complexes **2-5** indicate that the cells were not actively proliferating during the period of compound administration.

Microscopic study

HeLa cells were treated with 0.5 µM of cisplatin and complex **2-5** and incubated for 12 hrs to detect cellular survival. The treated and untreated cell debris were washed thrice with PBS and viewed under a light microscope (Zeiss). Survived HeLa cells are shown in Fig. 4.

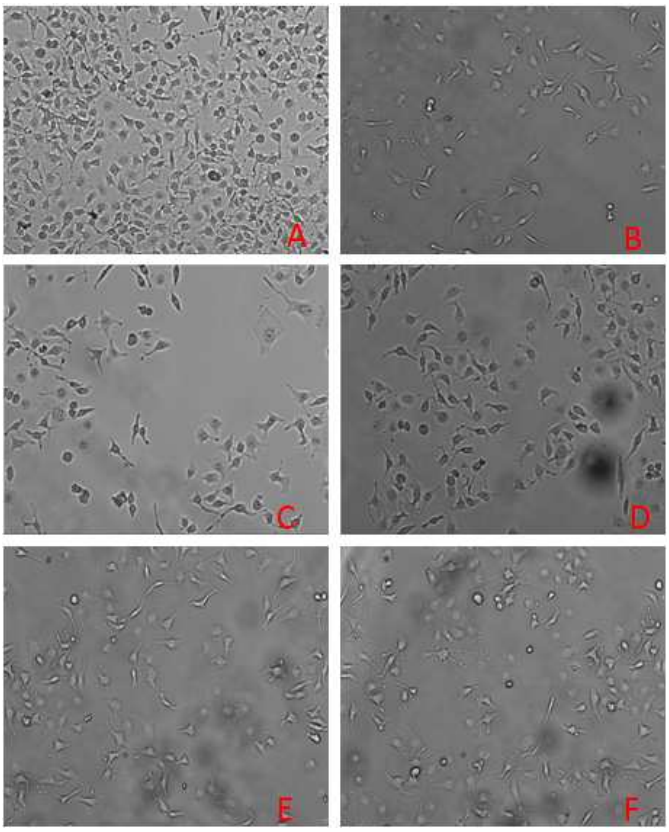

Fig. 4: Morphological changes of cell death: (A) cells treated without any complex; (B) with 0.05 µM of cisplatin; treated with 0.05 µM of (C) complex 2; (D) complex 3; (E) complex 4 and (F) complex 5 for 12 h.

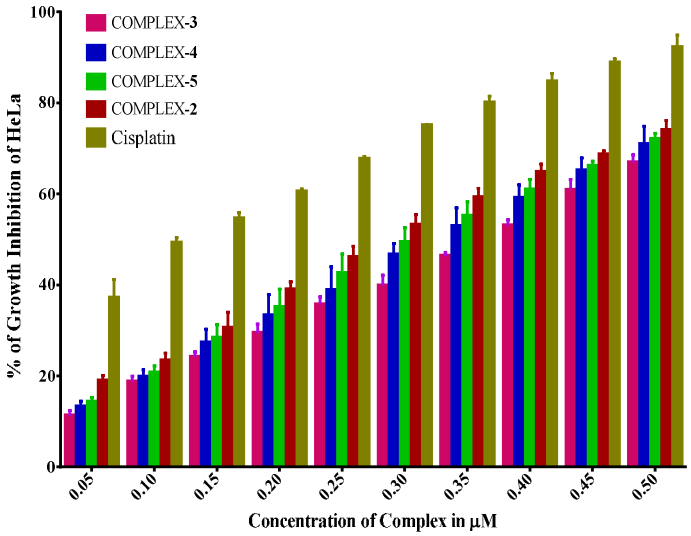

Fig. 5. % of growth Inhibition of Hela cell in presence of 2 and its substituted complexes 3, 4 and 5 concentration from 0.05 µM to 0.5 µM compared with cisplatin

DNA interaction studies with the complexes 2 to 5 by agarose gel electrophoresis

To observe DNA binding and degradation property of Pd(II) complexes, plasmid DNA was incubated with the various complexes. The control was maintained without treating with any of the complexes and electrophoretically run in the 0.8% agarose gel and the band pattern was observed. Mobility of plasmid DNA in lanes 2–8 is slightly degraded compared to lane-1 (control DNA). This result suggests that all the compounds including cis-platin have binding affinity to plasmid DNA (Fig. 6).

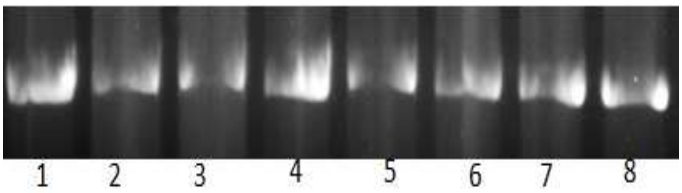

Fig.6. 0.8 % Agarose gel electrophoresis pattern of the pCDNA3. Lane 1 is Control not treated with any complex. Lanes 2 to 5 are DNA treated with complex-2, complex-3, complex-4, complex-5 in 0.05 µM concentration and the lanes 6 to 8 are DNA treated with complex-3, complex-4, complex-5 in 0.1µM concentration

Interestingly, the plasmid DNA interacted with the complexes and was cleaved by different concentrations of the complexes within 1 min incubation time.

Molecular docking with B-DNA

Molecular docking studies were carried out to obtain a theoretical insight into the interaction between complex **2** and B-DNA. The optimized structure of the metal complex **2** was docked with a B-DNA (taken from PDB) structure using HEX software[43]. The docked model[44] results suggest that palladium complex **2** binds with the minor groove of the B-DNA (Fig. 7). The complex **2** formed two hydrogen bonds with the Adenine ($3.2A^0$) through pyridine nitrogen and water is bonded with cytosine bases($3.2A^0$) of the 3' to 5' polynucleotide chain in B- DNA and total free energy of binding is -31.86 kcal/mol. The almost planar structure of the complex fits into the minor groove of the DNA in a parallel manner with respect to the DNA backbone. Therefore both the experimental DNA interaction results and computational docking data collectively suggest that **2** is a DNA groove binder.

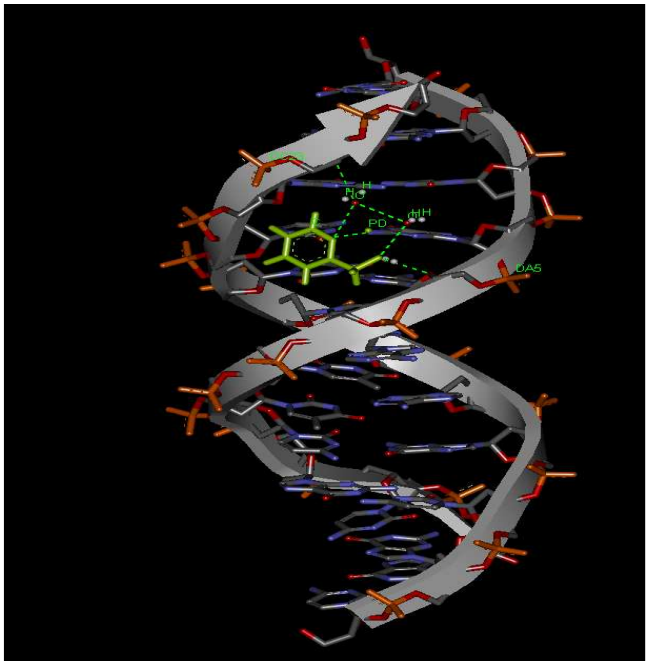

(A)

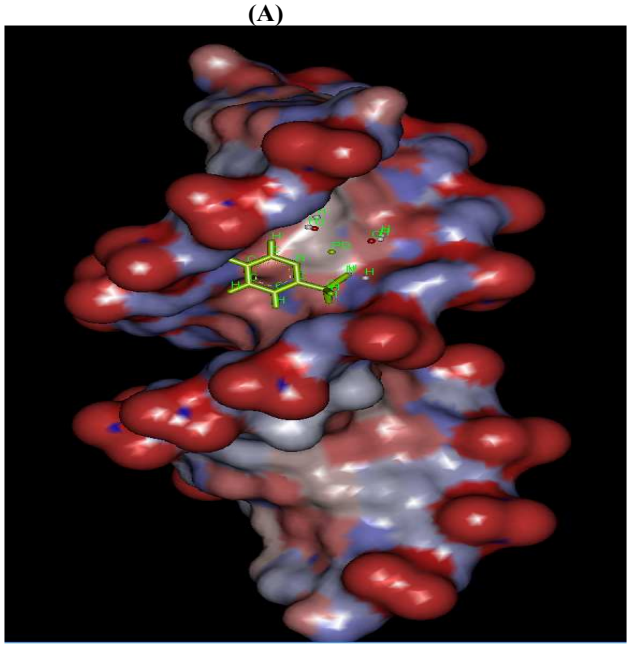

(B)

Fig.7. (A) Computational docking model (using the HEX software) of interaction between 2 and B-DNA (PDB ID:1BNA). (B) Magnified view of the interaction between 2 and DNA.

Conclusions

The kinetic and mechanistic studies reveal that the selected ligands: DL-meth, L-cys and N-ac-L-cys have significant affinity towards complex **2**, which is important for drug reservoir mechanism of thiols/thio-ethers in vitro with Pd(II) complexes. An associative mechanism is proposed which proceeds through an associative T.S via sulfur chelation along with simultaneous hydrogen bond

formation of the thiol protons (in case of L-cys/N-ac-L-cys) with bridged hydroxyl group. The more negative entropy of activation for both the steps implies enhanced ordering which is in good agreement with the kinetic data. The low enthalpy value is in consonance with a good degree of ligand participation in the transition state. The activation parameters ($\Delta H^{\ddagger}$ and $\Delta S^{\ddagger}$) strongly suggest an associative mode of activation. It can be concluded that the variation in size, bulkiness and electronic effect of the entering thiols reflect in their properties. Moreover, it is interesting to note that the reactions follow the unique third order kinetics. The reactivity order of the ligands is L-cys >DL-meth >N-ac-L-cys. This clearly demonstrates that the versatile kinetic behavior is controlled by steric and electronic effect as well as the donor property of oxygen and sulfur containing ligands, which is good agreement with SHAB principle.

Complex **2-5** possess significant antibacterial and anticancer properties. In vitro chemo sensitivity evaluation of the Pd(pic) complexes indicated that the cells were not actively proliferating during the period of complex administration. Complex **2-5** show anticancer activity of more or less 65-70 % on HeLa cells at higher concentration (0.05 μM) in comparison with cisplatin, which is remarkable. The Pd(pic) complexes show both antibacterial and anti cancer activity most likely by interacting with DNA in a similar way as cisplatin. To develop superior antibacterial and anticancer drug, these compounds can be used as start up for antibacterial agents and chemotype respectively. The computational molecular docking model suggests that complex **2** interacts with the minor groove of B-DNA. The almost planar structure of the complex **2** fits into the minor groove of the DNA in a parallel manner with respect to the DNA backbone.

Acknowledgements

The authors are thankful to National Institute of Technology Durgapur, W.B. 713209, DST, Government of India for providing financial assistance (Project No. SB/EMEQ-028/2013) and Vienna University of Technology, Vienna, Europe for providing the necessary assistance for carrying out this work. Thanks to Prof. A. K. Ghosh,University of Burdwan, WB, India for his valuable suggestion.

Address

a. Department of Chemistry, National Institute of Technology, Durgapur, Durgapur-713209, W.B., India
b. Institute of Applied Synthetic Chemistry, Vienna University of Technology, Getreidemarkt, 9/163 AC, A-1060 Vienna, Austria.
c. Department of Bio-Tech, National Institute of Technology, Durgapur-713209, W.B. India.

**Corresponding author's E.*mail: sankarmoi67@yahoo.com

References

1. J. Reedijk, Chem. Rev., 1999, **99**, 2499.
2. E. Wong and C. M. Giandomenico *Chem. Rev.* 1999**, 99***,* 2451
3. B. Lipert, Cisplatin. Chemistry and Biochemistry of a leading Anticancer Drug, ed., Wiley-VCH. Zürich/Weinheim 1999, 808.
4. E. Wong and C. M. Giandomenico, Chem. Rev. 1999, **99,** 2451.
5. G. Zhu, M. Myint, W.H. Ang, L. Song and S.J. Lippard, Cancer Res 2012, **72**,790.
6. P. M. Takahara, C. A. Frederick and S. J. Lippard, J. Am. Chem. Soc. 1996, **118**, 12309.
7. K.S. Lovejoy, et al. Proc Natl Acad Sci USA 2008, **105**, 8902.
8. N.J. Wheate, S. Walker, G.E. Craig and R Oun, Dalton Trans. 2010, **39,** 8113.
9. Y.W. Jung and S.J. Lippard, Chem Rev. 2007, **107,** 1387;
10. J. Kozelka, F. Legendre, F. Reeder and J. C. Chottard*,* Coord. Chem. Rev. 1999, **190,** 61.
11. G. Y. Park, J. J. Wilson, Y. Song, and S. J. Lippard, PNAS Early Edition 2012, 1.
12. A.S. Abu-Surrah, H.H. Al-Sadoni and M.Y. Abdalla, Cancer Therapy 2008, **6**, 1.
13. D. Wang and S. J Lippard, Nat. Rev. Drug. Discov. 2005, **4**, 307.
14. J. L. Butour, S. Wimmer, F. Wimmer and P. Castan, Chemico-Biological Interactions, 1997, **104,** 165.
15. A. C. F. Caires, Anti-Cancer Agents in Medicinal Chemistry, 2007, **7,** 484.
16. A. Garoufis, S. K. Hadjikakou and N. Hadjiliadis, Coord. Chem. Revs., 2009, **253,** 1384.
17. A. Samanta, G.K. Ghosh, I. Mitra, S. Mukherjee, J. C. Bose K., S. Mukhopadhyay, W. Linert and S.C. Moi, RSC Adv. 2014, **4,** 43516.
18. M. Curic, L .Tusek-Bozic, D. Vikic-Topic, V. Scarcia, A. Furlani, J. Balzarni and E. Declercq, J Inorg. Biochem. 1996, **63,** 125.
19. Z.Trávnek, L. Szuová and I. Popa, J Inorg Biochem, 2007, **101,** 477.
20. A. El-Sherif, M.M. Shoukry and R. van Eldik, Dalton Trans. 2003, 1425.
21. T. Rau, M. Shoukry and R. Van Eldik, Inorg. Chem. 1997, **36,** 1454.
22. R. W. Hay and A. K. Basak, J. Chem. Soc., Dalton Trans. 1982, 1819.

223. E. Gao , C. Liu , M. Zhu , H. Lin , Q. Wu and L. Liu, Anticancer Agents Med Chem. 2009, **3,** 356.
24. J.M. Andrews, J Antimicrob Chemother Suppl. 12001, **48**, 5.
25. A. Bolhuis, L. Hand, J. E. Marshall, A. D. Richards, A. Rodger, J and A. Wright, Eur. J. Pharm. Sci. 2011, **42,** 313.
26. R.W. Masters, Animal cell culture, Cytotoxicity and viability assays. 3rd Ed. 2000, 202.
27. C.Y. Sasaki, A. Passaniti, Bio-techniques, 1998, **24,** 1038.
28. J. L. Tian, E. Q. Gao, Y. T. Li and S. X. Liu, Synth. React. Inorg. Met.-Org. Chem. 1995, **25,** 417.
29. M. Chandrasekharan, M.R. Udupa and G. Aravamudan, Inorg. Chim. Acta, 1973, **7**, 88.
30. T. Z. Huyskens, H. Ratajczak and W. J. Orville-Thomas (eds) Mir, Moscow: Molecular Interactions, 1984, 17.
31. K.Nakamoto, IR and Raman spectra of Inorg. & Coord. Comps, Part B. J. Wiley, pp. 67.
32. R. Illavarasi, M.N.S Rao and M.R. Udupa, Indian J. Chem. 1998, **38A** 161.
33. G.Watt and D. S. Klett, Inorg. Chem. 1966, **5,** 1278.
34. J. Fujita, A.E. Martell and K. Nakamotom J. Chem. Phys, 1962, **36,** 324.
35. R.A. Condrate and K. Nakamoto, J. Chem. Phys, 1965, **42,** 2590.
36. R. M. Smith and A. E. Martin, Critical Stability Constants, (Plenum Press, New York*)*, 1989, 21.
37. T. M. Hui and T. C. Chou, The AAPS Journal. 2006, **8,** 485.
38. E. P. Serjeant and B. Dempsey, Ionisation constant of organic acids in aqueous solution, 1979, New York, Pergamon Press Inc., IUPAC Chemical data series no.**23**, 154.
39. A. E Martell and R.M Smith, Critical stability constant*,* Vol **1** (Plenum press, New York) 1974.
40. S.A. Kurzeev, G.M. Kazankor and A.D. Rybov, Inorg. Chim. Acta*,* 2002, **340,** 192.
41. R. van Eldik, T. Asano and W. J Noble, Chem. Rev*,* 1989, **89,** 549.
42. M. Kotowski and R. van Eldik, In Inorganic High Pressure Chemistry, and Elsevier Science Publishers: Amsterdam, 1986, 219.
43. G. Macindoe, L. Mavridis, V. Venkatraman, MD Devignes and DW. Ritchie. Hex Server: an FFT-based protein docking server powered by graphics processors. Nucleic Acids Res. 2010; 38: doi: 10.1093/nar/gkq311., PubMed PMID: 20444869; PubMed Central PMCID: PMC2896144.
44. K. Suntharalingam, O. Mendoza, A. Alexandra Duarte, David J. Mann and R. Vilar, Metallomics, 2013, **5**, 514.